7-29-2003

Surface salt bridges modulate DNA wrapping by the Type II DNA-binding protein TF1

Anne Grove
Louisiana State University

Recommended Citation

Grove, A. (2003). Surface salt bridges modulate DNA wrapping by the Type II DNA-binding protein TF1. *Biochemistry, 42* (29), 8739-8747. https://doi.org/10.1021/bi034551o

Surface Salt Bridges Modulate DNA Wrapping by the Type II DNA-Binding Protein TF1[†]

Anne Grove*

Department of Biological Sciences, Louisiana State University, Baton Rouge, Louisiana 70803

Received April 8, 2003; Revised Manuscript Received May 15, 2003

ABSTRACT: The histone-like protein HU is involved in compaction of the bacterial genome. Up to 37 bp of DNA may be wrapped about some HU homologues in a process that has been proposed to depend on a linked disruption of surface salt bridges that liberates cationic side chains for interaction with the DNA. Despite significant sequence conservation between HU homologues, binding sites from 9 to 37 bp have been reported. TF1, an HU homologue that is encoded by *Bacillus subtilis* bacteriophage SPO1, has nM affinity for 37 bp preferred sites in DNA with 5-hydroxymethyluracil (hmU) in place of thymine. On the basis of electrophoretic mobility shift assays, we show that TF1−DNA complex formation is associated with a net release of only ∼0.5 cations. The structure of TF1 suggests that Asp13 can form a dehydrated surface salt bridge with Lys23; substitution of Asp13 with Ala increases the net release of cations to ∼1. These data are consistent with complex formation linked to disruption of surface salt bridges. Substitution of Glu90 with Ala, which would expose Lys87 predicted to contact DNA immediately distal to a proline-mediated DNA kink, causes an increase in affinity and an abrogation of the preference for hmU-containing DNA. We propose that hmU preference is due to finely tuned interactions at the sites of kinking that expose a differential flexibility of hmU- and T-containing DNA. Our data further suggest that the difference in binding site size for HU homologues is based on a differential ability to stabilize the DNA kinks.

The bacterial histone-like HU proteins belong to the family of Type II DNA-binding proteins and are dimeric proteins with significant sequence and structural homology. HU homologues have been shown both to participate in compaction of the bacterial nucleoid and to act as accessory factors in cellular functions, such as DNA replication, transposition, and recombination (*1*−*12*). The structure of HU from *Bacillus stearothermophilus* reveals a compact core of intertwined monomers from which two β strands extend to embrace a DNA helix (*13*−*15*). The structure of the homologous *Escherichia coli* Integration Host Factor (IHF)[1] in complex with DNA shows that highly conserved prolines at the tips of the DNA-embracing β strands mediate two sharp DNA kinks; the overall ∼160° DNA bend is induced by the two prolines intercalating between specific DNA base pair steps separated by 9 bp of duplex; DNA distal to the kinks is wrapped about the lateral sides of the protein (*16*). Binding properties of HU homologues are quite diverse, with reported binding sites between 9 and 37 bp, and affinities ranging between 5 and 300 nM, indicating optimization of binding properties for diverse cellular roles (*4, 5, 17*−*21*). The large difference in the length of reported binding sites has appeared difficult to reconcile with the extensive sequence and structural homology.

A very limited dependence on salt concentration for IHF−DNA complex formation was recently reported and interpreted to be the consequence of numerous intramolecular surface salt bridges that must be broken to permit contacts to the DNA (*22, 23*). The hypothesis is that disruption of such salt bridges is required to create the cationic protein surface for DNA wrapping, unmasking cationic side chains, and permitting their participation in hydrated ion pairs with DNA phosphates (4−6 Å charge separation; *22, 23*). Upon DNA binding, release of cations previously associated with the negatively charged DNA backbone occurs, and anionic side chains, previously participating in surface salt bridges, now hydrate and accumulate atmospheres rich in cations (*24*). The disruption of surface salt bridges, manifested as a limited salt dependence of binding, would be expected to characterize DNA wrapping by other HU homologues as well.

The *B. subtilis* bacteriophage SPO1, whose genomic DNA is characterized by the complete substitution of thymine with 5-hydroxymethyluracil (hmU), encodes a HU homologue, TF1, which binds to 37 bp preferred sites within the SPO1 genome (*25, 26*). We have previously shown that TF1 binding sites are defined explicitly by the presence of two hmU−A base pair steps, corresponding to the two sites of proline-mediated DNA intercalation (*27, 28*). The wrapping of 37 bp of duplex about TF1 requires a lysine residue (Lys3) that contacts DNA 8−9 bp distal to the sites of kinking; Lys3 is critical, presumably because it secures DNA distal to the sites of kinking at positions that allow maximum leverage (*29*). We demonstrate here that complex formation by TF1 is only very modestly salt dependent and that removal of a surface-exposed anionic side chain can result in a slightly

[†] Supported by Louisiana Board of Regents Support Fund (LEQSF-(2000-03)-RD-A-07 to A.G.).

* Department of Biological Sciences, Louisiana State University, Baton Rouge, LA 70803. Tel: (225) 578-5148. Fax: (225) 578-8790. E-mail: agrove@lsu.edu.

[1] Abbreviations: hmU, 5-hydroxymethyluracil; IHF, Integration Host Factor; HBsu, *Bacillus subtilis* HU; TmHU, *Thermotoga maritima* HU.

10.1021/bi034551o CCC: $25.00
Published on Web 06/28/2003

increased salt dependence of binding for TF1, consistent with the proposal that disruption of surface salt bridges is linked to DNA wrapping. In the course of this analysis, a TF1 mutant protein was also generated whose DNA-binding properties suggested a mechanism for the discrimination between hmU- and T-containing DNA that is a hallmark of TF1. We suggest that the preference for hmU- over T-containing DNA is the result of a finely tuned interaction beyond the sites of kinking that exposes a differential flexibility of hmU−A and T−A base pair steps. Further, we propose that the length of the binding site engaged by HU homologues is determined by the ability of the particular protein to stabilize the proline-mediated DNA kinks.

EXPERIMENTAL PROCEDURES

Protein Preparation. Anionic residues targeted for mutagenesis were identified from the TF1 structure; potential salt bridges were identified by rotation of side chains using Swiss-PdbView. TF1 mutant proteins were generated by PCR amplification of plasmid pTF1X, carrying the wild-type TF1 gene (a gift from E. P. Geiduschek), using a forward primer designed to introduce the appropriate substitution at positions 13 or 90 of TF1 and a reverse primer positioned to abut the forward primer (primer sequences available on request). The PCR reaction, carried out with a mixture of Taq and Pfu polymerase, generated a full-length plasmid containing the mutated TF1 gene. The original template DNA was removed by *Dpn* I digestion, and the plasmid harboring the mutated TF1 gene was used to transform *E. coli* BL21(DE3)pLysS. Introduction of the desired mutation was confirmed by sequencing.

Purified wild-type TF1 was a generous gift from E. P. Geiduschek. Overexpression and purification of TF1−D13A was accomplished as described for TF1 (*27*). For TF1−E90A and TF1−E90A−A88D, cell lysates were fractionated by ammonium sulfate precipitation as described (*27*). The precipitate formed with 75% ammonium sulfate was dissolved in buffer A (20 mM Tris-HCl, pH 7.5, 50 mM KCl, 5% (v/v) glycerol, 1 mM EDTA, 0.2 mM phenylmethylsulfonyl fluoride, 3.5 mM 2-mercaptoethanol), dialyzed extensively against buffer A, and applied to a CM-Sepharose column equilibrated in buffer A. The proteins were eluted with a linear gradient from 50 mM to 1 M KCl in buffer A. Peak fractions were purified by chromatography on phenyl-Sepharose, as described (*27*). Purity was ascertained by Coomassie blue-staining of SDS-polyacrylamide gels. Protein concentrations were determined from the absorbance at 280 nm, using an extinction coefficient of 1200 M^{-1} for the TF1 monomer which contains a single tyrosine, except for TF1−E90A whose concentration was determined by quantitation of Coomassie blue-stained SDS-polyacrylamide gels, using wild-type TF1 as a standard.

Thermotoga maritima HU (TmHU) was generated as described (*21*). The *T. maritima* HU mutant protein, TmHU−V61F, was generated by PCR amplification of plasmid pET−TmHU carrying the gene encoding wild-type TmHU, using the approach described above for generation of TF1 mutant proteins (primer sequences available on request). Integrity of the clone was confirmed by sequencing. Overexpression and purification was accomplished as described for wild-type TmHU (*21*).

Glutaraldehyde Cross-Linking of TF1. Proteins (2 μg) were cross-linked in a total volume of 10 μL of 10 mM phosphate buffer, pH 7.0, with 0.1% glutaraldehyde at room temperature for 30 min. Reactions were terminated by addition of an equal volume of Laemmli sample buffer, and the cross-linked products were analyzed on 17% SDS-PAGE gels.

Electrophoretic Mobility Shift Assays Using Agarose Gels. Supercoiled or *Eco*RI-linearized pUC18 (100 ng) was mixed with TF1 in 10 μL binding buffer (20 mM Tris-HCl, pH 8.0, 0.1 mM EDTA, 0.1 mM dithiothreitol, 0.05% Brij58, 10 μg/mL BSA, 5% glycerol) with 100 mM KCl. The entire reaction was loaded on a 0.5% agarose gel in TBE (45 mM Tris-borate (pH 8.3), 1 mM EDTA). DNA was visualized by ethidium bromide staining following electrophoresis.

Preparation and Labeling of DNA Probes. Oligonucleotides with hmU content were provided by L. Mayol (*27, 30*). T-containing oligonucleotides were purchased and purified by denaturing polyacrylamide gel electrophoresis. The top strand was ^{32}P-labeled at the 5′ end with T4 polynucleotide kinase. Equimolar amounts of complementary oligonucleotides were mixed, heated to 90 °C, and slowly cooled to 4 °C to form duplex DNA.

Electrophoretic Mobility Shift Assay and Quantitation of Protein−DNA Complexes. Electrophoretic mobility shift assays were performed using 10% (w/v) polyacrylamide gels (39:1 acrylamide:bisacrylamide) in TBE supplemented with 10 mM NaCl (*27*). Gels were prerun for 30 min at 20 mA at room temperature before loading the samples with the power on. DNA and protein were incubated at room temperature for 45 min in binding buffer with the indicated concentration of KCl, NaCl, or potassium acetate, and each sample contained 5 or 10 fmol DNA in a total reaction volume of 10 μL unless specified otherwise. Under these conditions, binding equilibrium was reached before gel loading. Note that samples were loaded with the power on, such that separation began immediately after loading, limiting the ability of protein−DNA complexes to respond to the new electrolyte concentrations of the electrophoresis buffer. After electrophoresis, gels were dried, and protein−DNA complexes were visualized and quantified by phosphorimaging, using software supplied by the manufacturer (ImageQuant 1.1).

Equilibrium dissociation constants, K_d, were determined from the slope of Scatchard plots of DNA titrated with protein (*27*). Assuming binding to a single site and introducing the degree of binding as $[TF1]_B/[DNA]_T$, the Scatchard equation yields $[TF1]_B/([DNA]_T[TF1]_F) = K_a - K_a[TF1]_B/[DNA]_T$, where $[TF1]_B$ and $[TF1]_F$ are the concentrations of bound and free TF1, respectively, $[DNA]_T$ is the total concentration of DNA, and K_a is the equilibrium association constant. This method of determining K_d does not require correction for dissociation of protein−DNA complexes during electrophoresis; such correction would involve adjusting the fractional complex formation $[TF1]_B/[DNA]_T$ by an exponential decay factor representing complex dissociation during electrophoresis and would not change the slope of the Scatchard plot.

Linked ion release was calculated using a simple linkage relationship. For the interaction of TF1 with DNA to form the TF1·DNA complex, the reaction is characterized by the observed association constant $K_a = [TF1{\cdot}DNA]/([TF1]-$

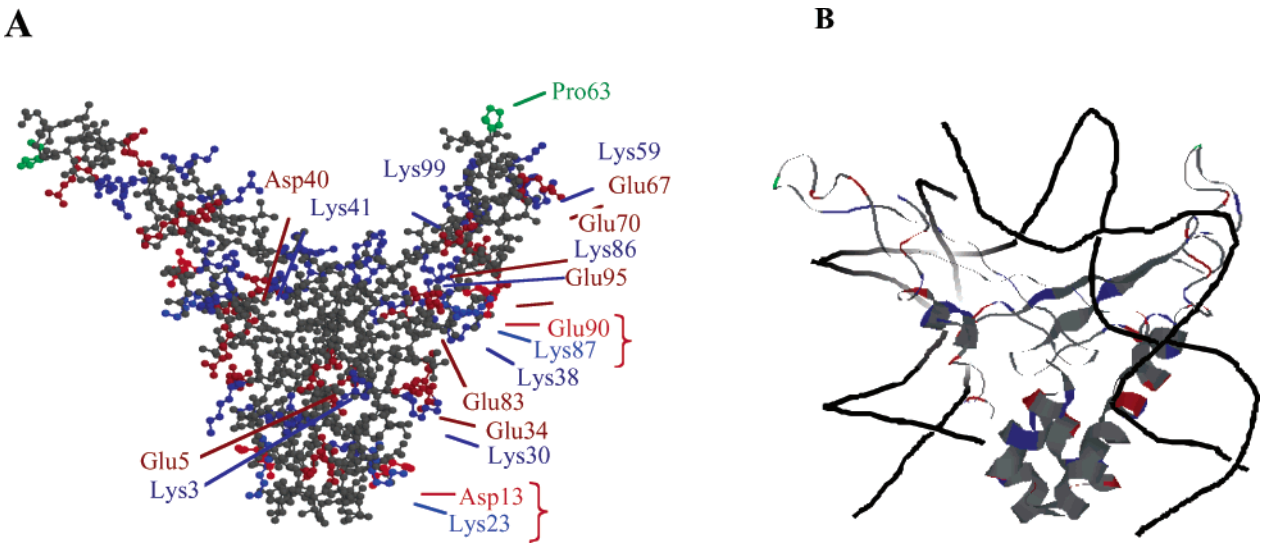

FIGURE 1: TF1 surface salt bridges. (A) Numerous surface salt bridges may be identified from the structure of the dimeric TF1 (*33*; PDB accession number 1WTU). Side chain rotations allow nine cationic residues from each subunit to form salt bridges with adjacent carboxylate groups. Such pairs include Lys3−Glu5, Lys23−Asp13, Lys30−Glu34, Lys38−Glu95, Lys41−Asp40, Lys59−Glu67, Lys86−Glu70, and Lys87−Glu90; the presence of Lys3 and Lys86 in the DNA-wrapping path was confirmed by mutagenesis experiments (*29*). In addition, Lys99 can form a salt bridge with Asp96 (obscured from view in this representation). Asp13 and Glu90 are highlighted with brackets, along with their potential salt-bridging partners. The DNA-intercalating Pro63 is identified (green). (B) Putative DNA-wrapping path. The DNA backbone corresponding to the DNA from the IHF−DNA complex (*16*; PDB accession number 1IHF) is overlaid on the uncomplexed structure of TF1. In a complex, the flexible β strands would refold to permit Pro63 from each subunit (green) to intercalate between two T−A base pair steps, separated by 9 bp of duplex. In this view, the β strand at the left would embrace the DNA from the front to allow intercalation at the DNA nick; for the β strand at the right, Pro63 would reach from the back of the DNA. A putative-wrapping path is specified down the right of the body of the protein (potential salt bridges highlighted in panel A). Lysine and arginine, blue; aspartate and glutamate, red; the DNA-intercalating Pro63, green. Illustration generated with RasMol.

[DNA]). This observed association constant is a function of solution variables (pH, $[K^+]$, etc.) As any interaction of ions, such as K^+, with both TF1 and DNA would participate in the association of TF1 with DNA, the thermodynamic association constant would be defined in terms of both [TF1], [DNA], [TF1·DNA], and the concentration of solution variables. For a polyelectrolyte such as DNA, the number of thermodynamically bound counterions is determined by axial charge density such that the fraction Ψ of a monovalent cation M^+ is bound to each phosphate. Salt bridge formation in the presence of ligand (protein) would release Ψ cations per phosphate. In absence of other effects:

$$\frac{d(\log K_a)}{d(\log [M^+])} = -n\,\Psi$$

where n is the number of ion pairs between DNA and ligand and $\Psi = 0.88$ for DNA. Thus, the dependence of log K_a on log $[M^+]$ reveals the net number of ions released upon binding (*24*, *31*, *32*). Assuming a generally weak binding of anions, we may determine the net release of cations from this relationship. Observed binding constants are implied throughout. All experiments were carried out at least in triplicate. Fits to data points were performed using KaleidaGraph. Values are reported as the average ± the standard error of the mean.

RESULTS

Localization of Surface Salt Bridges. The solution structure of TF1, solved in 400 mM NaCl, is shown in Figure 1 (*34*). TF1, which exhibits the same overall structural features as *B. stearothermophilus* HU and IHF, has 12 Asp + Glu and 15 Arg + Lys residues per monomer distributed to generate a positive electrostatic potential across the top of the saddle-shaped structure from which two β strands emerge to interact with the central ~9 bp of the cognate DNA (*16*, *33*). Significant structural homology to IHF and similarity of DNA-binding properties in terms of affinity and length of binding site suggest that TF1 and IHF engage their DNA targets similarly. For TF1, no favored electrostatic potential for DNA interaction may be distinguished down the lateral sides of the body of the protein that would be expected to interact with DNA distal to the two proline-mediated DNA kinks (*33*). Rather, inspection of surface-exposed residues reveals that numerous cationic residues that may be in a position to form hydrated salt bridges with DNA phosphates (4−6 Å charge separation) can also form dehydrated surface salt bridges with neighboring anionic side chains (~3 Å charge separation) following allowable rotations of side chains (Figure 1A). One possible salt-bridged configuration involving cationic residues in the proposed wrapping path is shown in Figure 1A in which nine cationic residues from each subunit participate in salt bridges with adjacent carboxylate groups.

We elected to analyze the role of Asp13 which may form a dehydrated salt bridge with Lys23 of the opposite chain (Figure 1A). Removal of Asp13 would be expected to increase the salt dependence of binding, corresponding to a greater net release of cations, as interaction of Lys23 with DNA would no longer be linked to the hydration of Asp13. With prolines at the tips of the DNA-binding arms intercalating between the hmU−A base pair steps that define the binding site, and with distal DNA wrapping about the lateral sides of the protein in a largely B form conformation (*16*), Lys23 would be predicted to contact the ends of a 37 bp duplex.

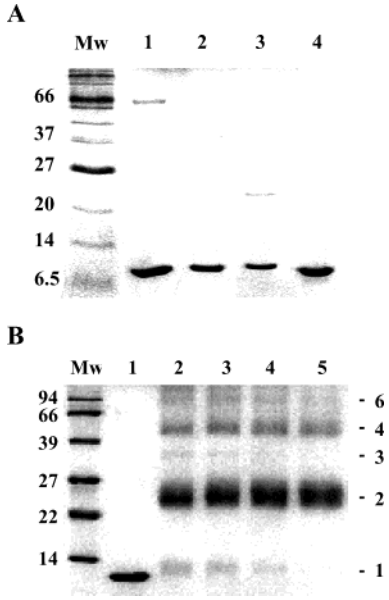

FIGURE 2: Purified TF1 and mutant proteins. (A) Coomassie blue-stained SDS-PAGE gel with lanes 1−4 containing 0.5−2 μg of TF1, TF1−D13A, TF1−E90A, and TF1−E90A−A88D, respectively. Small variations in electrophoretic mobility correlate with surface charge. Sample in lane 1 contains BSA. Molecular weight markers are shown at the left (in kDa). (B) Glutaraldehyde-mediated cross-linking of wild-type TF1 (2 μg). Lane 1 contains untreated TF1, lanes 2−5 contain TF1 cross-linked with glutaraldehyde in buffer containing 50, 100, 250, and 500 mM NaCl, respectively. Molecular weight markers are identified at the left (in kDa). Oligomeric assemblies are indicated at the right.

The IHF−DNA structure shows Lys86 interacting with DNA in the vicinity of the DNA kink (*16*). The corresponding residue in TF1 is flanked by Glu70, and the ~3.5 Å separation between these charged groups seen at 400 mM NaCl suggests a stable salt bridge (*33*). The neighboring Lys87 is flanked by both Glu83 and Glu90 and could form a dehydrated salt bridge with either (Figure 1A); like Lys86, Lys87 would be poised for interaction with DNA close to the proline-mediated DNA kink. We elected to substitute Glu90 with Ala with the expectation that Lys87 would form a surface salt bridge with Glu83, and that the salt dependence of binding for TF1−E90A would not differ significantly from that of wild-type TF1. Although the more polar Ser would be expected to be less disruptive as a surface-exposed residue, it has been shown to participate in hydrogen bonds to DNA; thus, both acidic residues were replaced with Ala which would not be expected to participate in contacts to DNA phosphates.

During preparation of TF1 mutant proteins, it became apparent that the replacement of Glu90 with Ala resulted in a TF1 variant with significantly increased affinity for T-containing DNA: transformants grew very slowly, and screening for transformants harboring the mutated pTF1−E90A plasmid also resulted in the isolation of TF1−E90A−A88D, in which the desired E90A substitution was combined with a substitution of Ala88 for Asp. Asp88, which may form a salt bridge with Lys87, thus restores the charge distribution of wild-type TF1. All mutant proteins, including the adventitiously generated TF1−E90A−A88D, were purified (Figure 2A). As shown for wild-type TF1 (Figure 2B), the predominant existence of dimers in solution depends only little on salt concentration. A slightly more efficient dimerization, evidenced by the disappearance of residual monomeric protein, is seen at higher salt concentrations, as expected for dimerization that is driven by hydrophobic interactions (*33*). Similar behavior is observed for all mutant proteins, consistent with an unaltered dimer interface (data not shown).

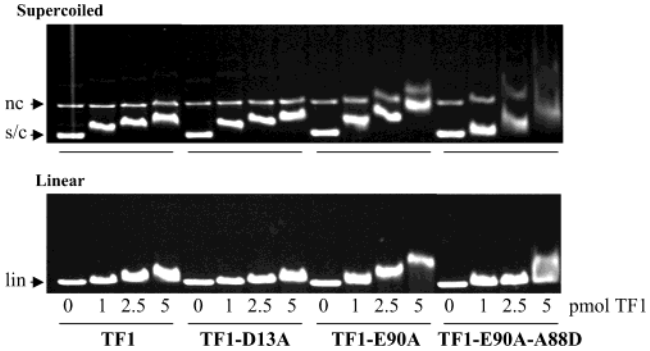

FIGURE 3: Agarose gel electrophoresis of TF1 variants binding to supercoiled (s/c; top panel; nc, nicked circle, identified by its sensitivity to digestion with exonuclease III) or linear DNA (lin; bottom panel). TF1 variants are identified at the bottom, and protein concentrations, identical for both panels, are indicated below the bottom panel.

DNA-Binding Properties of TF1 Mutants. Both wild-type TF1 and TF1−D13A bind preferentially to supercoiled DNA, as compared to linear DNA (Figure 3). This is also evidenced by the detection of a shift in mobility of the nicked circular DNA (nc) only at higher protein concentrations; preferred binding to supercoiled DNA is an expected property of TF1 which also binds preferentially to DNA distorted by the introduction of loops and bulges (*27, 28*). The preference for supercoiled DNA is lessened for TF1−E90A, which binds stably to all topological forms of the DNA. The higher affinity for DNA exhibited by TF1−E90A is attenuated in TF1−E90A−A88D, consistent with the spontaneous introduction of the A88D substitution in response to growth of *E. coli* harboring plasmid-expressing TF1−E90A. Consistent with high-affinity binding of TF1−E90A to DNA, a significant mobility shift is detected even after electrophoresis in the presence of ethidium bromide, whereas complexes involving wild-type TF1 and TF1−D13A are almost completely disrupted under these conditions (data not shown).

The affinity of TF1 variants for 37 bp DNA was compared. The sequence of the DNA probe represents the preferred TF1 binding site that overlaps the SPO1 early promoter P_E6 (Figure 4A). The size of the binding site was selected such that it would accommodate precisely one TF1 dimer; this consideration is necessary as TF1 can form nested complexes on longer DNA fragments (*27, 34*). Binding to the cognate hmU-containing DNA probe was compared to complex formation with the corresponding T-containing probe in which all hmU residues were replaced with thymine.

The 37 bp duplexes were used in electrophoretic mobility shift assays to analyze complex formation with the TF1 variants. Wild-type TF1 and TF1−D13A both fail to form stable complexes with the T-containing version of the DNA, but exhibit comparable, high affinity for the hmU-containing DNA; K_d = 2.9 and 3.4 nM for TF1 and TF1−D13A, respectively, in 100 mM KCl (Figure 4B). TF1−E90A has ~3-fold higher affinity for hmU-containing DNA (K_d = 1.0 nM). Notably, a marked increase in complex formation with the T-containing duplex is also evident. As demonstrated

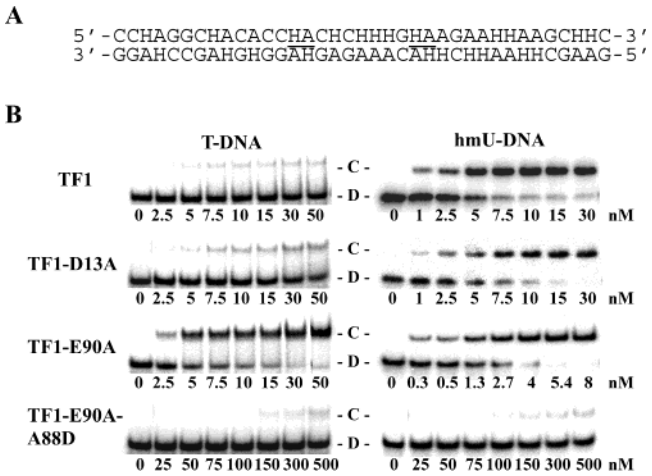

FIGURE 4: Electrophoretic mobility shift assay of TF1 variants binding to 37 bp T- or hmU-containing DNA. (A) Sequence of the preferred binding site for TF1, with the hmU−A base pair steps that define the binding site underlined; h stands for hmU. In the T-containing version, all hmU are replaced with T. (B) Titrations of T-containing DNA with TF1 variants (25 fmol DNA; left panel) and titrations of hmU-containing DNA with TF1 variants (10 fmol DNA; right panel). (C) Complex and (D) free DNA are identified between the panels. TF1 variants are identified at the left, and protein concentrations (in nM) are indicated below each panel.

previously, TF1 selects its preferred binding sites on the basis of inherent DNA flexure (*27*, *28*). Without the tandem hmU−A base pair steps that define the TF1 binding site, the T-containing duplex fails to provide the sites of enhanced DNA flexure requisite for stable complex formation with wild-type TF1 and TF1−D13A. The increased positive charge in the vicinity of the DNA kinks that characterizes TF1−E90A is apparently sufficient to permit complex formation with the less pliable T-containing DNA. The double-mutant protein, TF1−E90A−A88D, only exhibits measurable complex formation with the DNA probes at higher concentrations, no longer exhibiting preferred binding to hmU-containing DNA (Figure 4B).

Preferred Binding to hmU-Containing DNA. Almost all HU homologues feature three conserved residues, Arg−Asn−Pro, at the tips of the DNA-binding arms where the proline from each monomer intercalates between two base pair steps separated by 9 bp of duplex (*16*, *27*). In TF1, the Arg is replaced with Phe. It was previously reported that substitution of Phe with Arg rendered a TF1 mutant protein, TF1−F61R, with reduced site-selectivity in hmU-containing DNA and a marked increase in affinity for T-containing DNA (*35*). It was proposed that Phe may interact specifically with the hmU-containing DNA to confer selectivity. However, the comparable DNA-binding properties of TF1−F61R and TF1−E90A suggest that it is instead the greater positive charge in the vicinity of the DNA kinks that is responsible for the increased affinity for T-containing DNA. Consistent with this interpretation, we note that preference for hmU-containing DNA cannot generally be conferred simply by introducing Phe at position 61, as shown by the observation that introduction of Phe61 into the DNA-binding arms of HU from *T. maritima* yields a mutant protein, TmHU−V61F, with *reduced* affinity for hmU-containing DNA, as compared to wild-type TmHU (K_d = 4.4 ± 0.4 nM for TmHU and 18.7 ± 2.9 nM for TmHU−V61F).

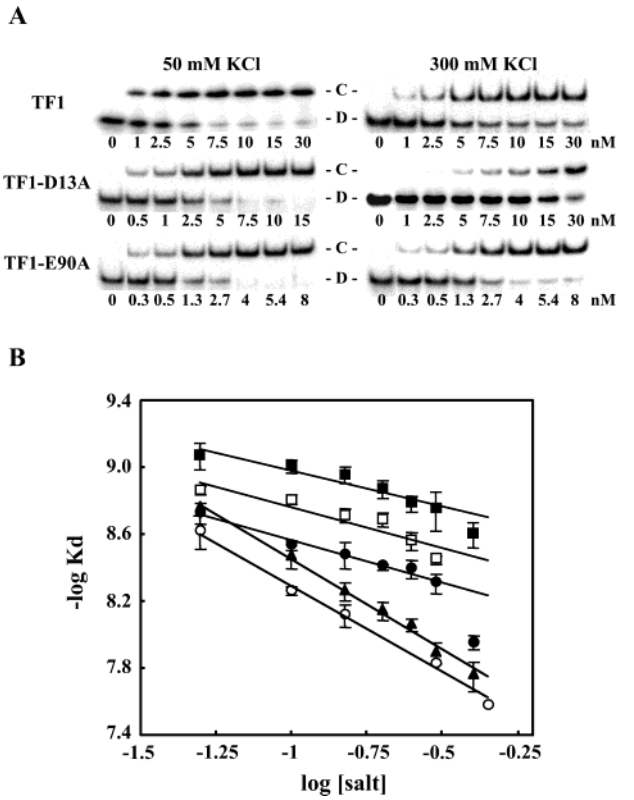

FIGURE 5: TF1−D13A exhibits greater salt-dependence of binding compared to wild-type TF1. (A) Titrations of hmU-containing DNA with TF1 variants at 50 mM KCl (left panel) and 300 mM KCl (right panel). (C) Complex and (D) free DNA are identified between the panels. TF1 variants are identified at the left, and protein concentrations (in nM) are indicated below each panel. (B) Thermodynamic linkage plots for TF1 variants. The slope of the lines reveals a net release of cations upon binding (for consistency, the linear portion of the plot is considered to correspond to 50−300 mM salt for all variants). (●) TF1 in KCl (n = 0.50 ± 0.04), (▲) TF1−D13A in KCl (n = 1.08 ± 0.05), (■) TF1−E90A in KCl (n = 0.42 ± 0.06), (○) TF1 in NaCl (n = 1.02 ± 0.05), (□) TF1 in potassium acetate (n = 0.48 ± 0.12).

Salt-Dependence of TF1−DNA Interactions. The affinity of TF1 variants for the 37 bp hmU-containing DNA was measured at different concentrations of KCl (Figure 5A). Notably, wild-type TF1 and TF1−D13A have equivalent binding affinities at low salt concentrations (50 mM KCl; Figure 5A, left panel), but complex formation with TF1−D13A is significantly reduced at higher salt concentrations (300 mM KCl; Figure 5A, right panel) compared to wild-type TF1. The electrophoretic mobility assay implies that binding equilibrium has been reached before sample loading. Because separation begins immediately upon loading, separation is expected to begin before protein−DNA complexes can adjust to the new ionic strength conditions; with a pI of 9.2 for wild-type TF1, free protein moves in the opposite direction of the protein−DNA complex. Furthermore, the comparable affinity of the TF1 variants suggests that any adjustment to the new buffer conditions would be comparable as well, indicating that differences in salt dependence indeed reflect solution conditions. For all TF1 variants, the negative slopes of the thermodynamic linkage plots indicate a net ion release associated with complex formation; the binding constant is approximately linearly dependent on salt concentrations at low to moderate concentrations of KCl, whereas the affinity may be significantly reduced at con-

centrations of KCl above ~300 mM (Figure 5B and data not shown). For TF1, an unusually modest dependence of K_d on [KCl] is evident, with a net release of only ~0.5 cations upon complex formation. To confirm the primary contribution of cations to the measured net ion release, the affinity of wild-type TF1 was also measured as a function of [NaCl]; if cations are largely responsible for the detected net ion release, then replacement of K^+ with the less mobile Na^+ ion would be expected to affect the measurements. This comparison is confirmatory of the expected, primary role of cations, as the much larger anions would be bound much less tightly (*24*, *42*). Affinities are generally lower when measured in NaCl, with a net release of ~1 cation (Figure 5B). A measurement of K_d as a function of potassium acetate yields affinities that are higher than in KCl, with a net ion release of ~0.5 cations. The very limited dependence of salt concentration on complex formation is the expected outcome if TF1 presents numerous surface salt bridges that must be disrupted concomitantly with complex formation. Substitution of Asp13 for Ala, predicted to disrupt a salt bridge between Asp13 and Lys23, indeed results in a slightly greater net release of cations compared to wild-type TF1, with an estimated net release of ~1 cation in KCl. In contrast, TF1−E90A, which exhibits a higher affinity than TF1 at all concentrations of KCl, forms DNA complexes with an associated net cation release that is not significantly different from that seen with wild-type TF1.

DISCUSSION

Disruption of Surface Salt Bridges Is Linked to Complex Formation. As both proteins and DNA interact with water and solutes, a complete understanding of protein−DNA complex formation requires measurement of binding affinity under different solution conditions (*32*, *36*−*38*). For example, the polyelectrolyte effect has served as a strong theoretical basis on which to interpret the dependence of protein−DNA complex formation on salt concentration. The polyelectrolytic nature of nucleic acids causes the local accumulation of counterions (e.g., Na^+, K^+), and binding of oligocations causes a partial neutralization of the negatively charged nucleic acid backbone with the concomitant release of counterions. For such oligocations, the observed equilibrium dissociation constant increases in response to an increase in salt concentration, with an estimate of the net number of cations released obtained from its dependence on salt concentration over the linear range (*39*−*41*). At low salt concentrations, such complex formation is primarily entropically driven as the counterion release that occurs upon oligocation−DNA binding provides the primary driving force for binding. For many proteins, analysis of binding to nucleic acids has also revealed a marked dependence of the binding constant on salt concentration, and the net number of cations released has often been interpreted in terms of the number of ion pairs involved in interaction with DNA. However, proteins that wrap DNA not only have positively charged residues in the wrapping interface but also a significant number of negatively charged side chains with which positively charged residues may form dehydrated surface salt bridges. As anionic side chains, previously engaged in surface salt bridges, hydrate and accumulate atmospheres rich in cations on complex formation, it follows that simple polyelectrolyte theory is insufficient to describe such complex formation and that the thermodynamic number of cations released cannot be simply correlated to the number of ion pairs involved in DNA interaction.

Extensive networks of surface salt bridges have been identified in several DNA-wrapping interfaces, including those of IHF, *E. coli* single-strand binding protein (SSB), and the nucleosome core particle (*22*, *23*). Similarly, analysis of surface residues of TF1 (Figure 1) reveals that a strikingly large number of anionic side chains are located near lysine or arginine residues that are predicted to participate in DNA wrapping (*33*). As proposed for IHF, the very limited salt dependence of TF1−DNA complex formation (Figure 5) suggests that an extensive network of surface salt bridges characterizes the DNA-wrapping interface of TF1. This interpretation is directly supported by the observation that modest changes in salt dependence result from substitution of an anionic residue (TF1−D13A; Figure 5) or from substitution of Na^+ for K^+. The slight differences in affinity measured in KCl or potassium acetate may reflect a preferred binding of Cl^- to TF1. The relatively greater ability of Cl^- than CH_3COO^- to lower binding affinity has also been observed for other DNA-binding proteins, including *E. coli* SSB, bacteriophage T4 gp32, and *E. coli* RNA polymerase (*42*−*44*). It is also important to note that very modest differences in affinity may be detected (e.g., by replacing Cl^- with CH_3COO^-), arguing for the ability of the electrophoretic mobility assay to reflect solution conditions appropriately.

The salt-bridge hypothesis provides a rationale for the presence of carboxylates within the DNA-wrapping path. The structure of IHF in complex with DNA shows the presence of several anionic residues in the vicinity of DNA phosphates. Five anionic side chains are within 6 Å of anionic DNA phosphate oxygen atoms and an additional nine are between 6 and 8 Å from phosphate oxygens (*16*, *22*). Likewise, anionic residues may be identified within the TF1 structure that may be close to DNA in a complex (Figure 1). If the proposed cationic salt-bridging partners associate with DNA phosphates, the carboxylates may still be close to the DNA as they take up cations from the solvent. Indeed, acidic residues have been suggested to bind cations that become part of the interface of a protein−DNA complex (*45*). In this circumstance, removal of the acidic residue resulted in the uptake of one less cation on formation of the complex. Analogously, it is conceivable that cations may be incorporated in the TF1−DNA interface and contribute to binding interactions.

It is formally possible that salt-dependent variations in protein oligomerization or intermolecular conformational changes may contribute to the observed salt dependence of binding and that such variations may be different for wild-type and mutant TF1. It is unlikely that significant changes in the oligomerization state occur under the conditions used in these experiments, as shown by cross-linking of TF1 at different ionic strengths (Figure 2 and data not shown). For TF1−E90A, conformational changes may indeed have resulted from the removal of Glu90, as evidenced by the altered substrate specificity of the mutant protein, and this altered structure may respond distinctly to changes in ionic strength. However, we note that an analysis of a potential contribution of conformational changes to the heat capacity changes recorded for IHF−DNA complex formation clearly

argue against conformational changes being solely responsible for the observed heat capacity changes (*22*).

Analysis of potential surface salt bridges suggested that Lys87 is in a position to form a salt bridge with either Glu90 or Glu83 (Figure 1A). The observation that the salt dependence of binding for wild-type TF1 and TF1−E90A is comparable indicates that an equivalent number of salt bridges are disrupted upon complex formation by both proteins. The following interpretations appear consistent with the observed binding properties. It is possible that Lys87 forms a salt bridge with Glu90 in wild-type TF1 and that it pairs with Glu83 in TF1−E90A, resulting in disruption of an equivalent number of salt bridges for the two proteins on complex formation. The different surface disposition of Lys87 that results from a change in a salt-bridging partner causes, in turn, an increased affinity for T-containing DNA. The introduction of Asp88 affords an alternate salt-bridging partner for Lys87, causing a severe attenuation of DNA binding. Differential surface disposition of Lys87 would then be the primary cause of the observed differences in DNA-binding properties of the mutant proteins. It may also be that Lys87 forms a salt bridge with Glu83 both in wild-type TF1 and in TF1−E90A. Glu90 may reside in the DNA-wrapping path in TF1, and its replacement with alanine removes an unfavorable interaction that causes increased binding to T-containing DNA. The second-site reversion may place Asp88 in the DNA-wrapping path or, more likely, form a salt bridge with Lys87 that results in unfavorable interactions between Glu83 and the DNA.

Discrimination between T- and hmU-Containing DNA. TF1 binds sequence specifically to hmU-containing DNA, with two hmU−A base pair steps serving as necessary and sufficient recognition sites for high-affinity binding. On the basis of comparison of TF1 binding to hmU-containing DNA, to hmU/T-copolymers and to T-containing DNA with loops, it was demonstrated that target site selection by TF1 is based on recognition of sequence-dependent DNA flexure, and that the two hmU−A base pair steps that define the binding site supply such flexure points (*27*, *28*). On the basis of DNA-binding properties and structural analyses, TF1 is expected to engage its DNA target similarly to IHF with Pro63 intercalating between the two hmU−A base pair steps to produce the DNA kinks (*16*, *25*, *27*−*29*, *33*−*35*, *46*, *47*).

The remarkable increase in affinity for T-containing DNA that characterizes TF1−E90A (Figures 3 and 4) suggests a molecular mechanism for the discrimination between hmU- and T-containing DNA. Because the only identifiable criterion for generation of a TF1-binding site is the presence of two DNA sites of higher than average flexure, we propose that discrimination between hmU- and T-containing DNA is achieved by means of protein contacts that suffice for binding and bending the more pliable hmU-containing DNA but that are insufficient for bending T-containing DNA. Accordingly, wild-type TF1 binds only hmU-containing DNA, and changes in the spatial disposition of charged residues, as seen for TF1−E90A−A88D (Figure 4), may abrogate binding even to hmU-containing DNA. Likewise, substitution of Lys86, predicted to contact DNA near the proline-mediated kinks, severely attenuates DNA binding (*29*). Notably, introduction of an additional positive charge in the vicinity of the DNA kinks, either through removal of Glu90 to which Lys87 may form a salt bridge (Figure 4) or through the replacement of Phe61 with Arg (*35*), provides sufficient stabilization of the DNA kinks, even in the less pliable T-containing DNA. We propose that preferred binding of hmU-containing DNA depends on precisely adjusted protein−DNA contacts that expose a differential flexibility between the two DNA substrates and that such distinguishing contacts must be made in the vicinity of the proline-mediated DNA kinks. For HU homologues that have evolved to stabilize DNA kinks in duplex T-containing DNA, for example, *T. maritima* HU, such differential DNA flexibility may go undetected, resulting in comparable binding affinities (*21*). In support of this analysis, we note that TF1 mutant proteins in which Phe61 is replaced with Ser or Gln fail to bind stably both to hmU-containing DNA and to T-containing DNA with sets of tandem mismatches (4 nt loops) at the positions of DNA intercalation. Only bulge loops, considered to impose a static kink on the DNA structure as opposed to the looser, more flexible conformation imposed by 4 nt loops, support complex formation with these defective mutant proteins as demands on stabilization of the DNA kinks are lessened (*28*). Taken together, analysis of TF1 mutants in which residues in a position to contact DNA near the proline-mediated kinks are altered supports the notion that the ability to engage a DNA target requires binding interactions that are sufficient to stabilize the kink and that discrimination between hmU- and T-containing DNA requires precisely adjusted interactions that suffice for bending of the more pliable hmU−A base pair steps but not T−A steps.

Notably, a TF1 mutant protein (TF1−E15G−T32I) with ~40-fold higher affinity than wild-type TF1 may be generated whose substitutions cause exposure of a positively charged patch on the protein surface in a region that contacts DNA beyond the ends of a 25 bp duplex (*27*, *46*, *47*). As the increased binding energy is manifested only with DNA longer than 25 bp, it must be due to contacts to the lateral sides of the protein. However, this mutant protein employs equivalent DNA contacts in the vicinity of the DNA kinks, and it retains preference for hmU−DNA. Evidently, although an overall increase in binding energy may enhance binding to T-containing DNA, the preference for hmU-containing DNA is not abrogated if the additional DNA contacts are far removed from the sites of kinking.

Length of the Binding Site Engaged by HU Homologues. Not all HU homologues wrap duplex DNA. For example, the *E. coli* HU heterodimer has been reported to engage only 9 bp of duplex (*17*). Yet, ~20 bp of DNA may be protected by *E. coli* HU if the DNA contains a nick or a four-way junction (*48*). It was also suggested that an ~65° bend at the nick or junction was required for *E. coli* HU to engage the longer DNA site and that an asymmetric disposition of HU with its β arm interacting at the nick/junction was the most probable mode of interaction (*48*). This would be equivalent to the interaction of IHF or TF1 with their respective half-sites, and it would argue that *E. coli* HU engages its DNA target similarly to IHF and TF1, provided that suitable flexure points are built into the DNA. Thus, we propose that HU homologues that are reported to engage only ~9 bp of duplex do so because they fail to stabilize the proline-mediated DNA kinks in duplex DNA, thereby precluding interaction between distal DNA and the lateral sides of the protein. Only if the DNA provides suitable points

of flexure or a predisposed DNA bend, as seen in nicked DNA or in four-way junction structures, can the severely bent DNA conformation be stabilized and a longer DNA target come into protein contact. Correspondingly, IHF can bind DNA without sequence specificity at low salt concentrations, with an estimated nonspecific binding site size of 9 bp at 60 mM KCl (*22*).

For TF1, the ability to distinguish between hmU- and T-containing DNA is required for selective regulation of phage-encoded genes through its specific binding to SPO1 early promoters. TF1, in its interaction with T-containing DNA, however, may not be significantly different from the host-encoded HU homologue, *B. subtilis* HU (HBsu). Both TF1 and HBsu bind nonspecifically and with low affinity to relaxed T-containing DNA but with preference for supercoiled DNA (Figure 3). The accumulation of TF1 during SPO1 infection is therefore not likely to interfere with host DNA functions. For some HU homologues, including *E. coli* and *B. subtilis* HU, nonspecific, low-affinity binding is considered the basis for their role in compaction of the bacterial nucleoid (*1*−*3*, *5*). However, the selective recognition of distorted DNA structures changes the mode of DNA interaction and permits preferred binding to such structures, possibly forming the basis for the reported roles of HU proteins in events such as repair and recombination (*6*−*12*). We propose that HU homologues utilize equivalent modes of DNA interaction with the ability to wrap longer DNA substrates dictated by optimization of residues involved in stabilization of the proline-mediated DNA kinks or by the presence of suitable flexure points in the DNA.

ACKNOWLEDGMENT

Helpful discussions with members of the Grove laboratory are gratefully acknowledged.

SUPPORTING INFORMATION AVAILABLE

Titrations of TmHu and TmHU−V61F with 37 bp T-containing DNA and hmU-containing DNA (PDF). This material is available free of charge via the Internet at http://pubs.acs.org.

REFERENCES

1. Drlica, K., and Rouvière-Yaniv, J. (1987) Histone-like protein of bacteria.*Microbiol. Rev. 51*, 301−319.
2. Kellenberger, E., and Arnold-Schultz-Gahmen, B. (1992) Chromatins of low-protein-content: special features of their compaction and condensation. *FEMS Microbiol. Lett. 100*, 361−370.
3. Oberto, J., Drlica, K., and Rouvière-Yaniv, J. (1994) Histones, HMG, HU, IHF: Même combat. *Biochimie 76*, 901−908.
4. Azam, T. A., and Ishihama, A. (1999) Twelve species of the nucleoid-associated protein from *Escherichia coli*. *J. Biol. Chem. 274*, 33105−33313.
5. Broyles, S. S., and Pettijohn, D. E. (1986) Interaction of the *Escherichia coli* HU protein with DNA. Evidence for formation of nucleosome-like structures with altered DNA helical pitch. *J. Mol. Biol. 187*, 47−60.
6. Huisman, O., Faelen, M., Girard, D., Jaffe, A., Toussaint, A., and Rouvière-Yaniv, J. (1989) Multiple defects in *Escherichia coli* mutants lacking HU protein. *J. Bacteriol. 171*, 3704−3712.
7. Dri, A. M., Moreau, P. L., and Rouvière-Yaniv, J. (1992) Role of the histone-like proteins Osmz and HU in homologous recombination. *Gene 120*, 11−16.
8. Boubrik, F., and Rouvière-Yaniv, J. (1995) Increased sensitivity to γ irradiation in bacteria lacking protein HU. *Proc. Natl. Acad. Sci. U.S.A. 92*, 3958−3962.
9. Aki, T., and Adhya, S. (1997) Repressor induced site-specific binding of HU for transcriptional regulation. *EMBO J. 16*, 3666−3674.
10. Fernandez, S., Rojo, F., and Alonso, J. C. (1997) The *Bacillus subtilis* chromatin-associated protein Hbsu is involved in DNA repair and recombination. *Mol. Microbiol. 23*, 1169−1179.
11. Li, S., and Waters, R. (1998) *Escherichia coli* strains lacking protein HU are UV sensitive due to a role for HU in homologous recombination. *J. Bacteriol. 180*, 3750−3756.
12. Bahloul, A., Boubrik, F., and Rouvière-Yaniv, J. (2001) Roles of *Escherichia coli* histone-like protein HU in DNA replication: HU-beta suppresses the thermosensitivity of dnaA46ts. *Biochimie 83*, 219−229.
13. Tanaka, I., Appelt, K., Dijk, J., White, S. W., and Wilson, S. (1984) 3-Å resolution structure of a protein with histone-like properties in prokaryotes. *Nature 310*, 376−381.
14. White, S. W., Appelt, K., Wilson, K. S., Tanaka, I. (1989) A protein structural motif that bends DNA**.** *Proteins: Struct., Funct., Genet. 5*, 281−288.
15. Vis, H., Mariani, M., Vorgias, C. E., Wilson, K. S., Kaptein, R., Boelens, R. (1995) Solution structure of the HU protein from *Bacillus stearothermophilus*. *J. Mol. Biol. 254*, 692−703.
16. Rice, P. A., Yang, S. W., Mizuuchi, K., and Nash, H. A. (1996) Crystal structure of an IHF-DNA complex: A protein-induced DNA U-turn. *Cell 87*, 1295−1306.
17. Bonnefoy, E., and Rouvière-Yaniv, J. (1991) HU and IHF, two homologous histone-like proteins of *Escherichia coli*, form different protein-DNA complexes with short DNA fragments. *EMBO J. 10*, 687−696.
18. Lavoie, B. D., Shaw, G. S., Millner, A., and Chaconas, G. (1996) Anatomy of a flexer-DNA complex inside a higher-order transposition intermediate. *Cell 85*, 761−771.
19. Liu, S.-T., Chang, W.-Z., Cao, H.-M., Hu, H.-L., Chen, Z.-H., Ni, F.-D., Lu, H.-F., and Hong, G.-F. (1998) A HU-like protein binds to specific sites within *nod* promoters of *Rhizobium leguminosarum*. *J. Biol. Chem. 273*, 20568−20574.
20. Kobryn, K., Naigamwall, D. Z., and Chaconas, G. (2000) Site-specific DNA binding and bending by the *Borrelia burgdorferi* Hbb protein. *Mol. Microbiol. 37*, 145−155.
21. Grove, A., and Lim, L. (2001) High-affinity DNA binding of HU protein from the hyperthermophile *Thermotoga maritima*. *J. Mol. Biol. 311*, 491−502.
22. Holbrook, J. A., Tsodikov, O. V., Saecker, R. M., and Record, M. T., Jr. (2001) Specific and non-specific interactions of integration host factor with DNA: thermodynamic evidence for disruption of multiple IHF surface salt-bridges coupled to DNA binding. *J. Mol. Biol. 310*, 379−401.
23. Saecker, R. M., and Record, M. T., Jr. (2002) Protein surface salt bridges and paths for DNA wrapping. *Curr. Opin. Struct. Biol. 12*, 311−319.
24. Record, M. T., Jr., Zhang, W., and Anderson, C. F. (1998) Analysis of effects of salts and uncharged solutes on protein and nucleic acid equilibria and processes: a practical guide to recognizing and interpreting polyelectrolyte effects, Hofmeister effects, and osmotic effects of salts. *Adv. Protein Chem. 51*, 281−353.
25. Greene, J. R., and Geiduschek, E. P. (1985) Site-specific DNA binding by the bacteriophage SP01-encoded type II DNA-binding protein. *EMBO J. 4*, 1345−1349.
26. Curran, J. F., and Stewart, C. R. (1985) Cloning and mapping of the SPO1 genome. *Virology 142*, 78−97.
27. Grove, A., Galeone, A., Mayol, L., and Geiduschek, E. P. (1996) On the connection between inherent DNA flexure and preferred binding of hydroxymethyluracil-containing DNA by the type II DNA-binding protein TF1. *J. Mol. Biol. 206*, 196−206.
28. Grove, A., Figueiredo, M. L., Galeone, A., Mayol, L., and Geiduschek, E. P. (1997) Twin hydroxymethyluracil-A base pair steps define the binding site for the DNA-binding protein TF1. *J. Biol. Chem. 272*, 13084−13087.
29. Grove, A., and Saavedra, T. C. (2002) The role of surface-exposed lysines in wrapping DNA about the bacterial histone-like protein HU. *Biochemistry 41*, 7597−7603.
30. Conte, M. R., Galeone, A., Avizonis, D., Hsu, V. L., Mayol, L., and Kearns, D. R. (1992) Solid-phase synthesis of 5-hydroxymethyluracil containing DNA. *Bioorg. Med. Chem. Lett. 2*, 79−82.

31. Lohman, T. M., and Mascotti, D. P. (1992) Thermodynamics of ligand-nucleic acid interactions. *Methods Enzymol. 212*, 400−424.
32. Record, M. T., Jr., Ha, J. H., and Fisher, M. A. (1991) Analysis of equilibrium and kinetic measurements to determine thermodynamic origins of stability and specificity and mechanism of formation of site-specific complexes between proteins and helical DNA. *Methods Enzymol. 208*, 291−343.
33. Jia, X., Grove, A., Ivancic, M., Hsu, V. L., Geiduschek, E. P., and Kearns, D. R. Structure of the *Bacillus subtilis* phage SPO1-encoded type II DNA-binding protein TF1 in solution. (1996) *J. Mol. Biol. 263*, 259−268.
34. Schneider, G. J., Sayre, M. H., and Geiduschek, E. P. (1991) DNA-bending properties of TF1. *J. Mol. Biol. 221*, 777−794.
35. Sayre, M. H., and Geiduschek, E. P. (1990) Effects of mutations at amino acid 61 in the arm of TF1 on its DNA-binding properties. *J. Mol. Biol. 216*, 819−833.
36. O'Brien, R., DeDecker, B., Fleming, K. G., Sigler, P. B., and Ladbury, J. E. (1998) The effects of salt on the TATA binding protein-DNA interaction from a hyperthermophilic archaeon. *J. Mol. Biol. 279*, 117−125.
37. Lohman, T. M., Overman, L. B., Ferrari, M. E., Kozlov, A. G. (1996) A highly salt-dependent enthalpy change for *Escherichia coli* SSB protein−nucleic acid binding due to ion−protein interactions. *Biochemistry 35*, 5272−5279.
38. Li, L., and Matthews, K. S. (1997) Differences in water release with DNA binding by ultrabithorax and deformed homeodomains. *Biochemistry 36*, 7003−7011.
39. Record, M. T., Jr., de Haseth, P. L., and Lohman, T. M. (1977) Interpretation of monovalent and divalent cation effects on the lac repressor-operator interaction. *Biochemistry 16*, 4791−4796.
40. Lohman, T. M., de Haseth, P. L., and Record, M. T., Jr. (1978) Analysis of ion concentration effects of the kinetics of protein-nucleic acid interactions. Application to lac repressor-operator interactions. *Biophys. Chem. 8*, 281−294.
41. Moraitis, M. I., Xu, H., and Matthews, K. S. (2001) Ion concentration and temperature dependence of DNA binding: comparison of PurR and LacI repressor proteins. *Biochemistry 40*, 8109−8117.
42. Overman, L. B., Bujalowski, W., and Lohman, T. M. (1988) Equilibrium binding of *Escherichia coli* single-strand binding protein to single-stranded nucleic acids in the $(SSB)_{65}$ binding mode. Cation and anion effects and polynucleotide specificity. *Biochemistry 27*, 456−471.
43. Lohman, T. M. (1984) Kinetics and mechanism of dissociation of cooperatively bound T4 gene 32 protein−single-stranded nucleic acid complexes. 2. Changes in mechanism as a function of sodium chloride concentration and other solution variables. *Biochemistry 23*, 4665−4675.
44. Leirmo, S., Harrison, C., Cayley, D. S., Burgess, R. R., and Record, M. T., Jr. (1987) Replacement of potassium chloride by potassium glutamate dramatically enhances protein−DNA interactions in vitro. *Biochemistry 26*, 2095−2101.
45. Bergqvist, S., O'Brien, R., and Ladbury, J. E. (2001) Site-specific cation binding mediates TATA binding protein−DNA interaction from a hyperthermophilic archaeon. *Biochemistry 40*, 2419−2425.
46. Andera, L., Spangler, C. J., Galeone, A., Mayol, L., and Geiduschek, E. P. (1994) Interrelations of secondary structure stability and DNA-binding affinity in the bacteriophage SPO1-encoded type II DNA-binding protein TF1. *J. Mol. Biol. 236*, 139−150.
47. Liu, W., Vu, H. M., Geiduschek, E. P., and Kearns, D. R. (2000) Solution structure of a mutant of transcription factor 1: implications for enhanced DNA binding. *J. Mol. Biol. 302*, 821−830.
48. Kamashev, D., Balandina, A., and Rouvière-Yaniv, J. (1999) The binding motif recognized by HU on both nicked and cruciform DNA. *EMBO J.18*, 5434−5444.

BI034551O